A Novel AC to AC Wireless Power Transfer System for EV Charging Applications

Erdem Asa, Jason Pries, Veda Galigekere, Subho Mukherjee, Omer C. Onar, Gui-Jia Su, and Burak Ozpineci
Power Electronics and Electric Machinery Group, Oak Ridge National Laboratory
National Transportation Research Center, Knoxville, TN 37932, USA
E-mail: asae@ornl.gov, priesjl@ornl.gov, galigekerevn@ornl.gov, mukherjees1@ornl.gov, onaroc@ornl.gov, sugj@ornl.gov, burak@ornl.gov

Abstract— **In this paper, a novel ac to ac wireless power transfer (WPT) system is introduced for electric vehicle (EV) charging applications to reduce cost and design complexity. The presented wireless power transfer concept achieves unity power factor (UPF) on the grid-side by using a hybrid frequency ac / ac converter without an additional converter stage and closed loop control compared to the conventional systems. Due to inherent merit of the proposed ac / ac converter, ac input with 60 Hz grid frequency can be directly transferred to the load by superimposing with high frequency switching signal through the wireless coils. To validate the theoretical analysis of the proposed WPT system, the experimental results of the proposed converter are provided for 650 W output power by using 6 inches air gap between the couplers with the input of 110 V_{RMS} ac source. The system overall efficiency is measured 89 % achieving 0.99 power factor (PF) and 1.5 % current total harmonic distortion (THD).**

Keywords—ac-to-ac converter, grid frequency, high frequency, wireless power transfer, EV / PEV charger

I. Introduction

Due to elimination of physical electrical contacts, wireless power transfer has several advantages in electric vehicle charging systems [1]. An EV charging system consists of two different charging points, ac and dc platforms in the car as shown in Fig. 1. As seen from the figure, WPT system is usually integrated to the dc charging platform that requires four power conversion stages, ac / dc and dc / ac out of the vehicle, ac / ac through the coupling coils, and ac / dc stage on the vehicle [2]. Single or three phase grid power is converted to dc in ac / dc stage that provides power factor correction and dc link voltage regulation at the output [3]-[4]. This stage might require larger dc link capacitors in order to operate at constant dc voltage. High frequency sinusoidal current is generated by dc / ac inverter and applied to the resonant stage and the primary coil and transmitted to the magnetically coupled pick-up coil. High frequency ac current in the secondary side coil is converted to the dc through ac / dc stage and used for charging the battery [5]-[6]. Considering the WPT system infrastructure from grid to the battery, a direct ac to ac system would be more cost effective without requiring the ac / dc conversion stage and the dc link with the bulky capacitor. Thus, a direct ac / ac WPT might be a good alternative for EV charging systems.

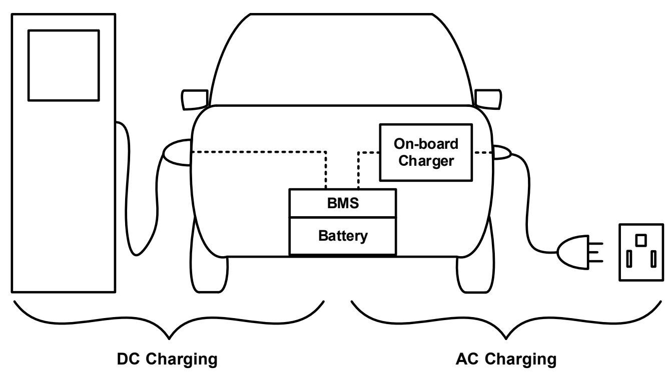

Fig. 1. PEV/EV charger system, ac and dc platforms.

Several single and three phase matrix converter topologies are explored to convert ac grid voltage to high frequency voltage in the literature [7]-[8]. Although their converter structure can eliminate the dc link, their configuration is complicated that usually employs bi-directional semiconductor switches and their circuit transient process is difficult and complex to analyze. Moreover, due to the signal chopping with complicated switching combinations, power quality of these systems is lower than the standard limitations. Single stage integrated ac / dc power factor correction (PFC) and dc / dc conversion topologies have also been investigated for WPT systems [9]-[10]. Although the overall system cost margin is reduced considering the single switch simplicity, these converters usually suffer from high

This manuscript has been authored by Oak Ridge National Laboratory, operated by UT-Battelle, LLC, under Contract No. DE-AC05-00OR22725 with the U.S. Department of Energy. The United States Government retains and the publisher, by accepting the article for publication, acknowledges that the United States Government retains a non-exclusive, paid-up, irrevocable, world-wide license to publish or reproduce the published form of this manuscript, or allow others to do so, for United States Government purposes. The Department of Energy will provide public access to these results of federally sponsored research in accordance with the DOE Public Access Plan (http://energy.gov/downloads/doe-public-access-plan).

voltage / current stresses that might be required in commutation or compensation circuits to reduce switching and conduction losses. Authors in [11] proposed a direct ac / ac converter to generate high frequency current on the primary side of a WPT system by using energy injection control to the load when it is needed. Proposed converter of Ref. [7] can reduce switching losses without reverse flow and a commutation circuit; however, the system input current THD is very high as shown from the experimental results. It might be convenient to inject the power to the load in a short period of time such as dynamic wireless charging applications, but the system may not be suitable to run continuously for stationary charging systems.

In this study, a novel hybrid frequency converter is proposed for EV charging applications. In this topology it is possible to have an open-loop controller without changing any control parameters such as frequency, phase shift, etc. With this property of the circuit, 60 Hz ac grid frequency can be converted to high frequency for use with the WPT. In the proposed hybrid frequency converter topology, half bridge lower and upper legs are driven with opposite gate signals during positive and negative half line cycles of the grid with 50 % duty cycle PWM. The simple topology provides a unique solution by reducing the system cost and ensures less complexity for ac / ac converter technologies, especially for WPT systems and EV chargers. Considering similar studies, the system THD can be reduced and PF can be improved with the proposed topology and front-end filter at the constant switching frequency. In order to prove the idea and demonstrated the operating principle, the system topology state model is analyzed, and theoretical analysis of the converter is presented. The system performance is validated with experimental results at 650 W output load with an input of 110 V_{RMS} ac source. From the results, the input power factor of 0.99 and input current THD of 1.5 % are achieved and the overall system efficiency is measured 89 % in the laboratory conditions. The efficiency is expected to be significantly higher at rated power levels compared to efficiency obtained at this low power level.

II. The Proposed Converter and System State Analysis

The proposed hybrid frequency ac / ac converter topology is shown for the WPT on-board chargers in Fig. 2. It comprises a front-end filter, series connected two half-bridge resonant inverters, a pair of coupling coils (or a closely coupled transformer in the case of a wired charger) with resonant capacitors, charger, and vehicle battery. The grid-side frequency and high frequency switching are superimposed through the coupling coils and fundamental frequency of the energy is transferred to the vehicle-side with a 60 Hz sinusoidal carrier signal. The converter state and switch transitions are presented the behavior of the proposed system in Figs. 3-6. To simplify the circuit analysis, filter losses are assumed to be negligible, the input capacitor is assumed to be large enough, and primary side active switches are ideal. The proposed circuit is analyzed when the grid sinusoidal voltage is in positive and negative half-cycles in the following operation modes, respectively.

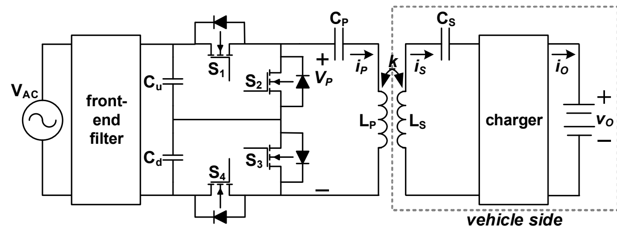

Fig. 2. The proposed ac/ac converter topology.

Mode 1 [t_0<t<t_1]

During this interval, the active switches S_1 and S_4 are turned on and body diode of switch S_3 is on-state when the grid voltage is in positive half-cycle. As shown in Fig. 3, the current flows through S_1, C_P, L_P, and S_4. Also, C_u is charged through S_4 and body diode of switch S_3 in the converter as depicted in Fig. 5.a. In negative half-cycle shown in Fig. 4, the current flows through S_4, L_P, C_P, and S_1. And, C_d is reverse charged through S_1 and body diode of switch S_2 as demonstrated in Fig. 6.a.

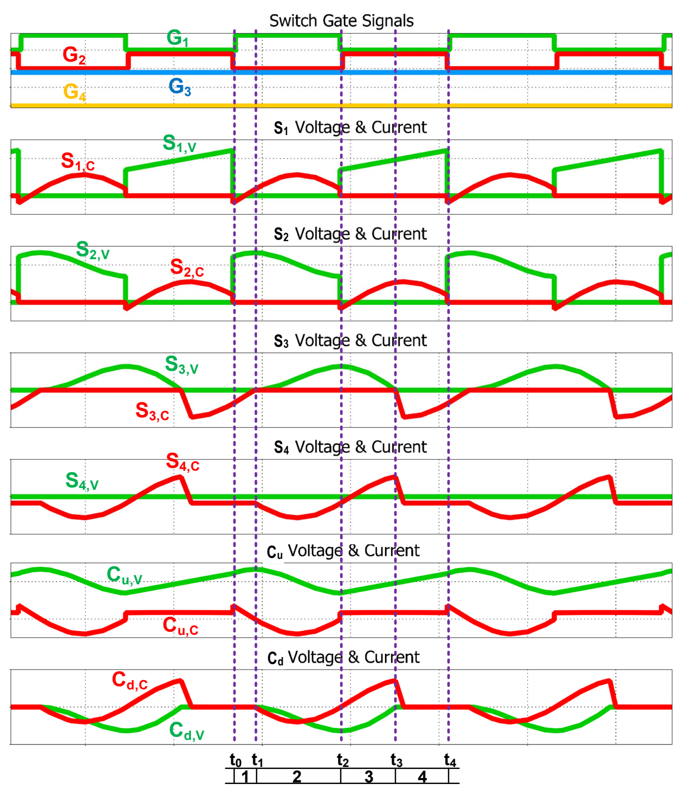

Fig. 3. Voltage and current waveforms of the switches, diodes, and capacitors during grid positive half-cycle.

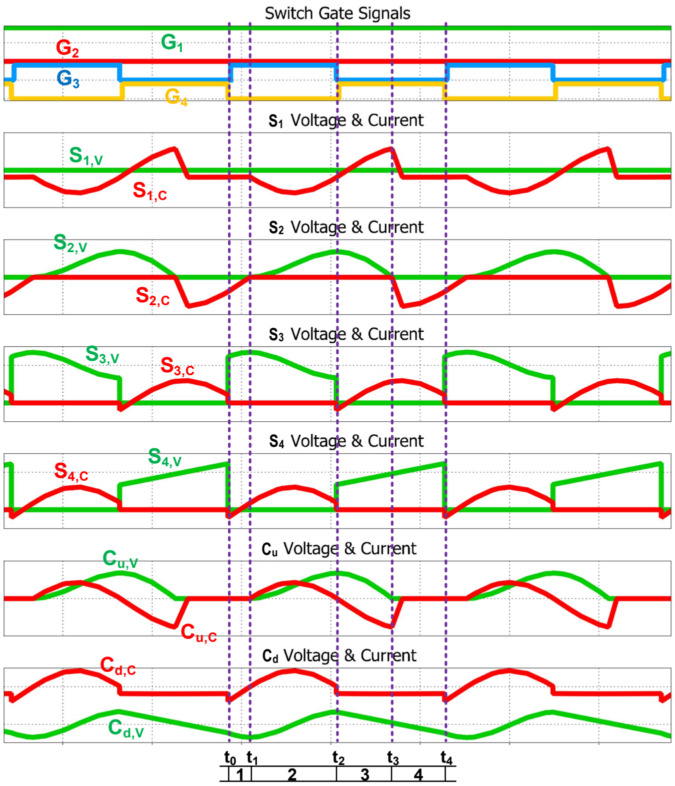

Fig. 4. Voltage and current waveforms of the switches, diodes, and capacitors during grid negative half-cycle.

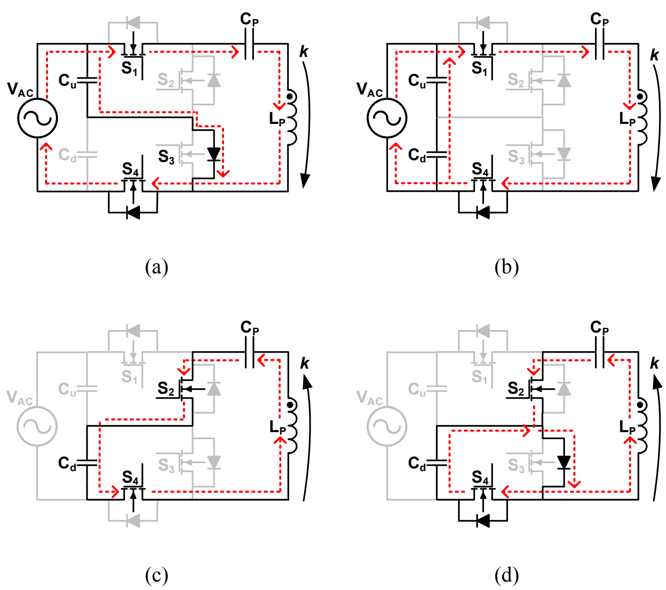

Fig. 5. Mode analysis, current path and switching transition during grid positive half-cycle.

Mode 2 [$t_1<t<t_2$]

In the positive half-cycle, the current flows through S_1, C_P, L_P, and S_4 as shown in Fig. 3 and Fig. 5.b. Also, C_d discharges and charges to C_u in opposite polarity in this state. In the negative half-cycle, the current is negative polarity and flows through S_4, L_P, C_P, and S_1 as shown in Fig. 4 and Fig. 6.b. Also, C_u discharges into C_d in this cycle.

Mode 3 [$t_2<t<t_3$]

The resonant tank current in L_P and C_P discharges through S_2, C_d, and S_4 during the positive cycle of grid voltage as plotted in Fig. 3 and Fig. 5.c. However, the resonant current in C_P and L_P circulates through S_1, S_3, and C_u when the grid voltage is in the negative half-cycle as shown in Fig. 4 and Fig. 6.c.

Mode 4 [$t3<t<t4$]

The resonant tank current flows through S_2, S_4, L_P, and C_P in the positive cycle of the grid voltage, and the capacitor C_d discharges through body diode of switch S_3 as shown in Fig. 3 and Fig. 5.d. The negative polarity of the grid voltage is demonstrated in Fig. 4 and Fig. 6.d. As seen from the negative interval state, the current flows through C_P, L_P, S_3 and the capacitor C_d discharges through body diode of switch S_4.

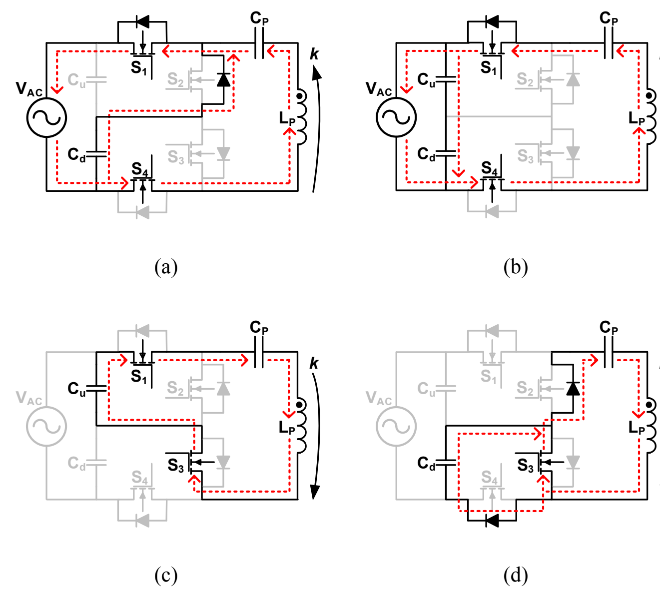

Fig. 6. Mode analysis, current path, and switching transition during grid negative half-cycle.

III. THE SYSTEM THEORETICAL ANALYSIS

As shown in Fig. 7, the WPT system model can be represented with an input voltage source V_i, resonant tuning capacitors C_P and C_S and, coupled inductors L_P and L_S with equivalent series resistances R_P and R_S, respectively. k is the coupling factor between the two coils such that leakage L_L and magnetizing inductance L_M values can be equivalently calculated from two coupled inductors as,

$$L_M = k\sqrt{L_P L_S} = kL \tag{1}$$

$$L_L = L - L_M = (1-k)L \tag{2}$$

where, both coils L_P and L_S are assumed to be identical and equal to L. Primary Z_P and secondary Z_S equivalent impedances, where

$$Z_P = \frac{1}{j\omega C_P} + R_P + j\omega L_L \tag{3}$$

$$Z_S = j\omega L_L + R_S + \frac{1}{j\omega C_S} \tag{4}$$

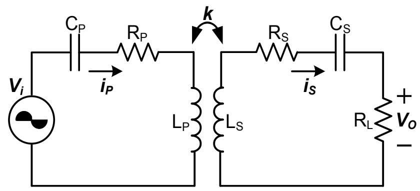

Fig. 7. Equivalent circuit of wireless power link.

Z_M is the magnetizing impedance related to the coupled inductors by $Z_M = j\omega L_M$. In these equations, $\omega = \{2\pi f_{sw}\}$ represents switching frequency of f_{sw}. The primary-side sinusoidal input voltage V_i is positive or negative, depending on the sign of the fundamental grid voltage with the frequency of f_{60} and can be defined as:

$$V_i(t) = \begin{cases} v_{i,max} sin(2\pi f_{60}), & 0 < \omega \leq \pi \\ -v_{i,max} sin(2\pi f_{60}), & \pi < \omega \leq 2\pi \end{cases} \tag{5}$$

Using the Kirchhoff's voltage law, primary and secondary resonant tank voltages in a matrix form can be written as

$$\begin{bmatrix} V_i \\ 0 \end{bmatrix} = \begin{bmatrix} Z_P + Z_M & -Z_M \\ -Z_M & Z_M + Z_S + R_L \end{bmatrix} \begin{bmatrix} I_P \\ I_S \end{bmatrix} \tag{6}$$

If the system is operated at the resonant frequency ω_R as where, $\omega_R = 1/\sqrt{L_P C_P} = 1/\sqrt{L_S C_S}$, the corresponding voltage and current transfer function of the WPT system can be written as,

$$|M_V| = \left|\frac{V_O}{V_i}\right| = \left|\frac{Z_P}{R_L} + \frac{Z_S(Z_P+Z_M)}{R_L Z_M} + \frac{Z_P+Z_M}{Z_M}\right|^{-1} \tag{7}$$

$$|M_I| = \left|\frac{I_S}{I_P}\right| = \left|\frac{Z_M}{Z_M+Z_S+R_L}\right| \tag{8}$$

IV. Experimental Results

The proposed ac / ac wireless system is validated for 650 W, 110 V_{RMS} ac input, and 110 V_{RMS} output voltage as a laboratory prototype. The WPT system is tested with 6-inch distance between coils which results in a coupling factor of 0.15. Primary coil dimensions are 28 inches by 28 inches and secondary coil dimensions are 15 inches by 19 inches, respectively. The power circuit hardware set-up diagram is given in Fig. 8.

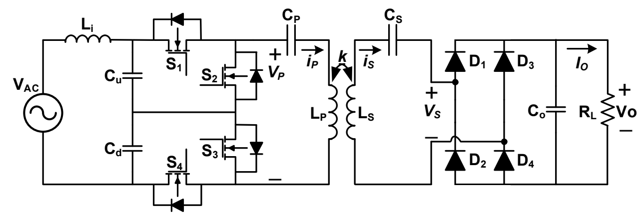

Fig. 8. The proposed converter experimental set-up diagram.

It's considered that the on-board charger has a rectifier stage with a unity power factor PFC inside. Thus, the system secondary is modelled through the rectifier and ohmic load as shown in laboratory set-up diagram. The corresponding parameters of the experimental setup are given in Table I. The characteristic waveforms of the proposed converter described in previous sections are given in the following records.

TABLE I

Symbol	Parameter	Value
V_{AC}	ac input voltage	110 V_{RMS}
V_O	output voltage	110 V_{RMS}
P_O	output power	650 W
L_i	input filter inductor	180 µH
C_u, C_d	decoupling capacitor	20 µF
C_P	primary resonant capacitor	47.76 nF
C_S	secondary resonant capacitor	40.8 nF
L_P	primary self-inductances	74.56 µH
L_S	secondary self-inductance	85.52 µH
k	coupling co-efficient	0.15
C_o	output capacitor	9 µF
f_{60}	grid frequency	60 Hz
f_{SW}	operating frequency	85 kHz
t_{dead}	dead time	500 ns

Fig. 9 (a) shows switch gate waveforms with grid 60 Hz sinusoidal voltage that S_1 and S_2 are 50 % duty complementary gate signals, S_3 is in on-state, and S_4 is in off-state in positive half-cycle. During the negative half-cycle, S_3 and S_4 gate signals are 50 % duty complementary, S_1 is in on-state, and S_2 is in off-state as demonstrated in Fig. 9 (b). The gate signal waveform data is collected using Tektronix MDO3024 mixed domain oscilloscope.

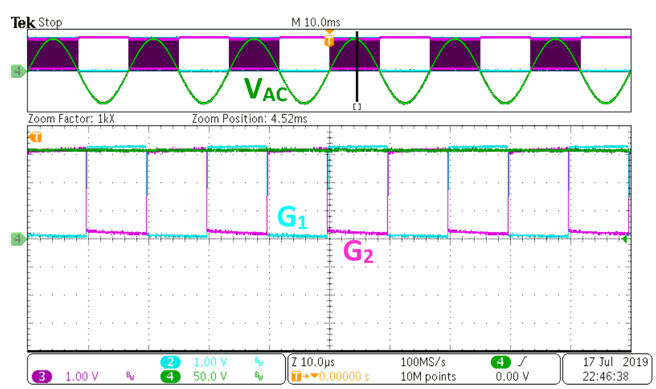

(a)

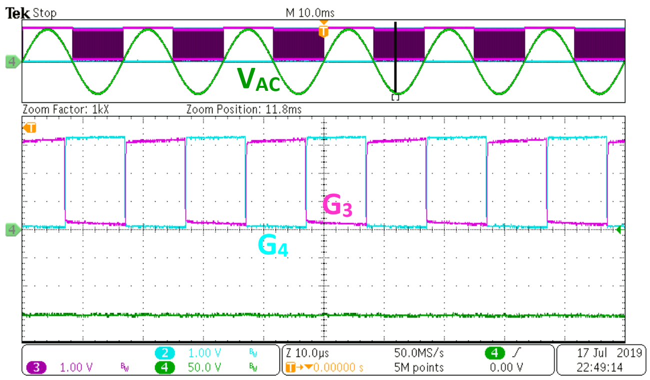

(b)

Fig. 9. The proposed converter modulation gate signals G_1, G_2, G_3, and G_4 (1 V / div) when the grid voltage V_{AC} (50 V / div) in a) positive half-cycle, and b) negative half-cycle [10 µs / div].

The input and output voltage / current waveforms are presented at 650 W load in Fig. 10. As seen from the figure, the system input voltage and current waveforms are purely sinusoidal, and the system input and output voltages are 110 V_{RMS}. The input ac source power factor and the input current THD are 0.9979 and 1.5 %, respectively. The overall efficiency of the system from the input ac source to the output load terminals is 89 %. The total conduction and switching losses are around 79 W and the input reactive power is 47 VAr. The grid frequency input and output waveforms are collected with a Yokogawa WT1806E precision power analyzer.

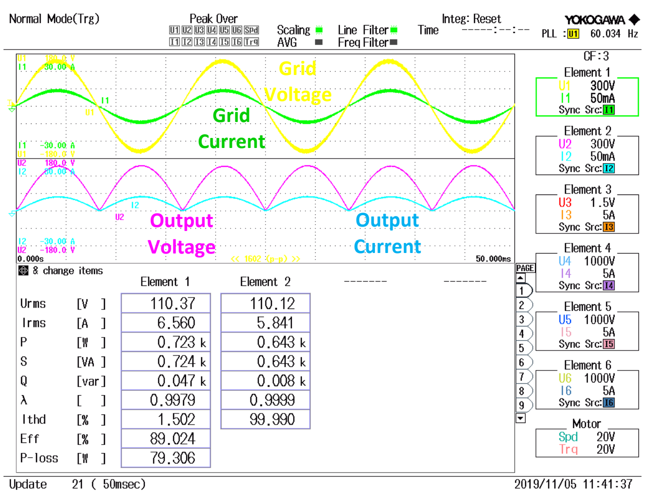

Fig. 10. The system input voltage V_{AC} and output voltage V_O (60 V / div), and input current i_{AC} and output current i_O (10 A / div) [5 ms / div].

The selected primary and secondary resonant tank voltage and current waveforms are given in Fig. 11 (a) with the switching frequency is constant at 85 kHz during grid 60 Hz frequency. Fig. 11 (b) and (c) present the zoomed-in waveforms during positive and negative half-cycles, respectively. As seen from the results, the system is running in open loop with 50 % duty cycle that the primary switches are ZVS during the operation in both positive and negative half-cycles. Moreover, the system current in primary and secondary sides are purely sinusoidal as seen from the waveforms. Teledyne Lecroy HDO8108 1GHz high-definition oscilloscope is used for data collection in this step.

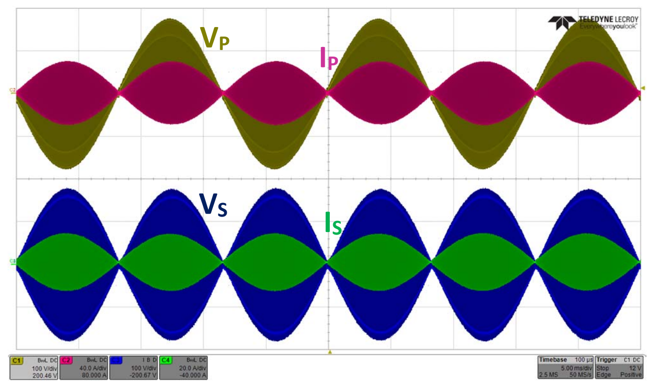

(a)

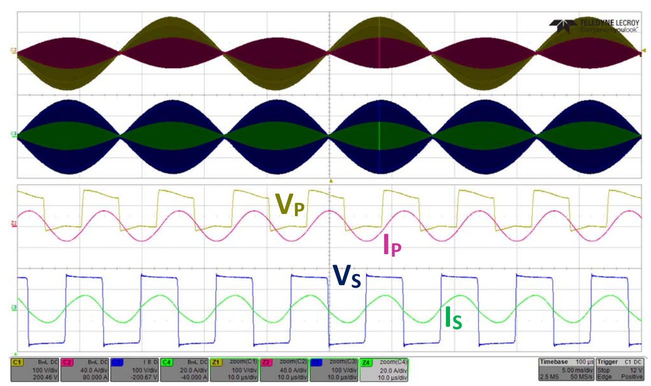

(b)

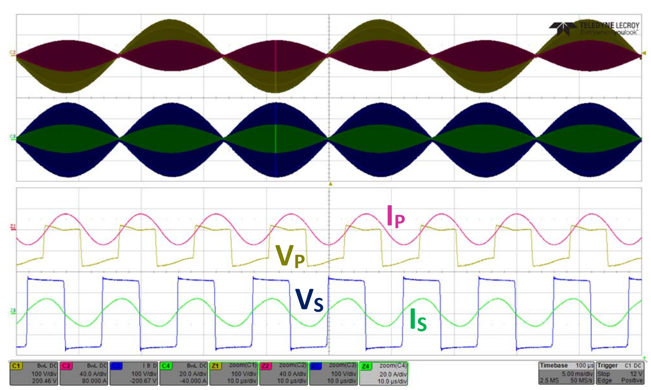

(c)

Fig. 11. The system experimental results; a) the system primary voltage V_P (100 V / div) and current i_P (40 A / div), and secondary resonant tank voltage V_S (100 V / div) and current i_S (20 A / div) waveforms during b) positive half-cycle, and c) negative half-cycle [100 us / div].

The proposed system comparison with conventional solutions is provided in Table II. The most significant achievement of the proposed system is the elimination of the bulky dc bus capacitors which reduces the weight, volume, and cost of the WPT power assembly. Furthermore, considering the system design requirements in WPT applications, the proposed solution reduces the system design process which is one of the most important aspects considering production engineering work.

TABLE II

	Conventional WPT		Proposed WPT
	Grid + Filter + Rectifier + Single Phase PFC + Half Bridge HF DC/AC + Wireless + Rectifier + Battery	Grid + Filter + Rectifier + Interleaved PFC + Full Bridge HF DC/AC + Wireless + Rectifier + Battery	Grid + Filter + Single Phase Hybrid DC/AC + Wireless + On-board Charger + Battery
FET	3	6	4
Diode	9	10	0
dc Bus Capacitor	1	1	0
Design Stages	2	2	1

V. CONCLUSIONS

In this study, a new ac / ac converter topology is presented for wired or wireless EV charging system. State analysis and analytic equations of the converter are described by the switch state conditions. Grid and output voltage and current waveforms are presented with primary and secondary resonant tank voltage and current waveforms at 60 Hz and 85 kHz frequencies. The experimental results are performed with 110 V_{RMS} ac input voltage and 110 V_{RMS} output voltage. It is demonstrated that the grid voltage at 60 Hz frequency can be converted to high-frequency ac voltage required for wireless power transfer with the proposed ac / ac hybrid frequency converter. The other important result is that the designed converter can be operated with constant frequency without requiring closed-loop control or additional converter stages. The output power of 650 W is observed at 89 % efficiency and obtained with 0.99 power factor and 1.5 % current THD. The efficiency is expected to be much higher at rated power as the experimental setup was operated at a much lower power than the rated in this initial proof of concept stage.

REFERENCES

[1] O. Onar, V. P. Galigekere, J. Pries, G. J .Su, S. Zou, S. Anwar, J. Wilkins, R. Wales, L. Seiber, C. White, "Modeling, Design, and Experimental Verification of a WPT Level-3 Wireless Charger with Compact Secondary Coupler," 2019 IEEE Applied Power Electronics Conference and Exposition (APEC), Anaheim, CA, USA, 2019, pp. 1722-1729.

[2] O. C. Onar, M. Chinthavali, S. L. Campbell, L. E. Seiber, C. P. White and V. P. Galigekere, "Modeling, Simulation, and Experimental Verification of a 20-kW Series-Series Wireless Power Transfer System for a Toyota RAV4 Electric Vehicle," 2018 IEEE Transportation Electrification Conference and Expo (ITEC), Long Beach, CA, 2018, pp. 874-880.

[3] M. Bojarski, E. Asa, K. Colak, D. Czarkowski, "A 25 kW Industrial Prototype Wireless Electric Vehicle Charger," IEEE Applied Power Electronics Conference and Exposition (APEC), Long Beach, CA, 2016, pp. 1756-1761.

[4] M. Bojarski, E. Asa, K. Colak, D. Czarkowski, "Analysis and Control of Multiphase Inductively Coupled Resonant Converter for Wireless Electric Vehicle Charger Applications," IEEE Transactions on Transportation Electrification, vol. 3, no. 2, pp. 312-320, June 2017.

[5] E. Asa, K. Colak, D. Czarkowski, "Analysis of Cascaded Multi-Output-Port Converter for Wireless Plug-in Hybrid/On-Board EV Chargers," IEEE Applied Power Electronics Conference and Exposition (APEC), Long Beach, CA, 2016, pp. 1323-1328.

[6] K. Colak, M. Bojarski, E. Asa, D. Czarkowski, "A Constant Resistance Analysis and Control of Cascaded Buck and Boost Converter for Wireless EV Chargers," IEEE Applied Power Electronics Conference and Exposition (APEC), Charlotte, NC, 2015, pp. 3157-3161.

[7] M. Moghaddami and A. I. Sarwat, "Single-Phase Soft-Switched AC–AC Matrix Converter With Power Controller for Bidirectional Inductive Power Transfer Systems," in IEEE Transactions on Industry Applications, vol. 54, no. 4, pp. 3760-3770, July-Aug. 2018.

[8] S. Weerasinghe, U. K. Madawala and D. J. Thrimawithana, "A Matrix Converter-Based Bidirectional Contactless Grid Interface," in IEEE Transactions on Power Electronics, vol. 32, no. 3, pp. 1755-1766, March 2017.

[9] J. Liu, W. Xu, K. W. Chan, M. Liu, X. Zhang and N. H. L. Chan, "A Three-Phase Single-Stage AC-DC Wireless-Power-Transfer Converter with Power Factor Correction and Bus Voltage Control," IEEE Journal of Emerging and Selected Topics in Power Electronics, *Early Access*.

[10] J. Liu, K. W. Chan, C. Y. Chung, N. H. L. Chan, M. Liu and W. Xu, "Single-Stage Wireless-Power-Transfer Resonant Converter With Boost Bridgeless Power-Factor-Correction Rectifier," in IEEE Transactions on Industrial Electronics, vol. 65, no. 3, pp. 2145-2155, March 2018.

[11] H. L. Li, A. P. Hu and G. A. Covic, "A Direct AC–AC Converter for Inductive Power-Transfer Systems," in IEEE Transactions on Power Electronics, vol. 27, no. 2, pp. 661-668, Feb. 2012.